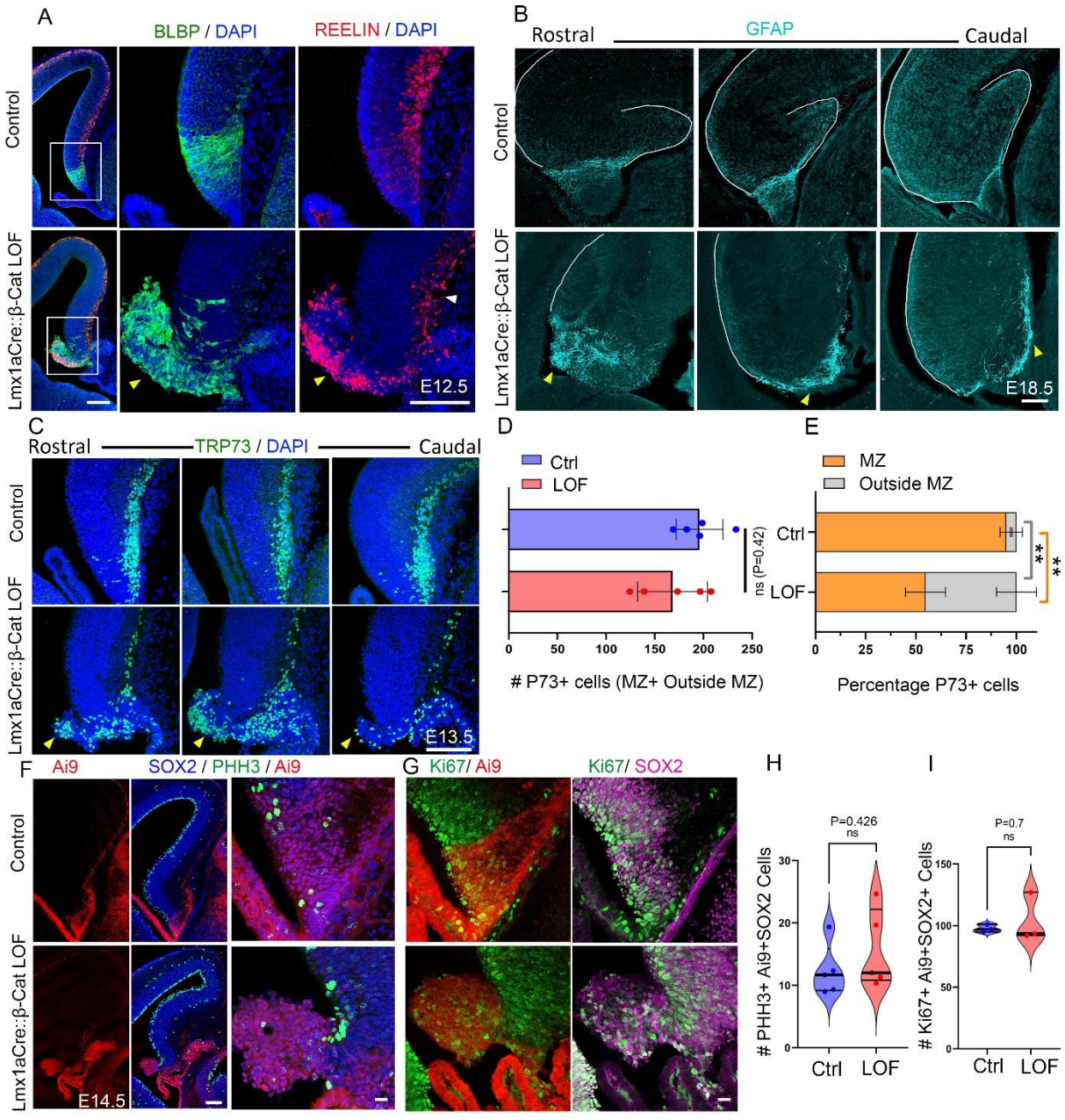

Fig. S1. Loss of β-CATENIN in the cortical hem causes dysmorphia of the fimbrial scaffold and mispositioning of the CR cells. (A) Co-immunolabeling for REELIN and BLBP at E12.5 reveals a disorganized fimbrial scaffold and mislocalized CR cells in Lmx1aCre::β-Catenin LOF brains compared with controls. These images show the individual BLBP (green) and REELIN (red) channels of the image in Fig. 2C). (B) GFAP labeling at E18.5 reveals a well-ordered fimbrial scaffold in controls, but a disorganized

scaffold in the Lmx1aCre::β-Catenin LOF brains (yellow arrowheads) at multiple rostro caudal levels; N=3 brains (biologically independent replicates) examined over 2 independent experiments. (C) A rostro caudal series reveals that TRP73+ hem-derived CR cells are mislocalized to the ectopically protruding glial mass (yellow arrowheads) throughout the rostro caudal extent of the E13.5 brain. (D) A bar graph representing the total number of TRP73+ cells (Mz+ Outside Mz) shows no significant difference between Lmx1aCre::β-Catenin LOF and control brains. (E) A stacked percentage bar graph displays the altered distribution of TRP73+ cells in Lmx1aCre::β-Catenin LOF compared to controls; N=5 (D and E) brains (biologically independent replicates) examined over 4 independent experiments, bars represent mean±SEM. (F, G) Co-immunostaining for proliferation markers PHH3 and Ki67, and progenitor marker SOX2 (H, I) Violin plots showing quantification of number of PHH3+SOX2+Ai9+ cells (H) and Ki67+SOX2+Ai9+ cells (I) reveal no change in proliferation in Lmx1aCre::β-Catenin LOF brains. Statistical tests (D, E, H and I): Two-tailed unpaired Mann Whitney U test, * $p < 0.05$, ** $p < 0.01$, *** $p < 0.001$, ns if p-value> 0.05; P=0.42 (D), P=0.0079 (E), P=0.426 (H), and P=0.7 (I). All scale bars: 100 μm.

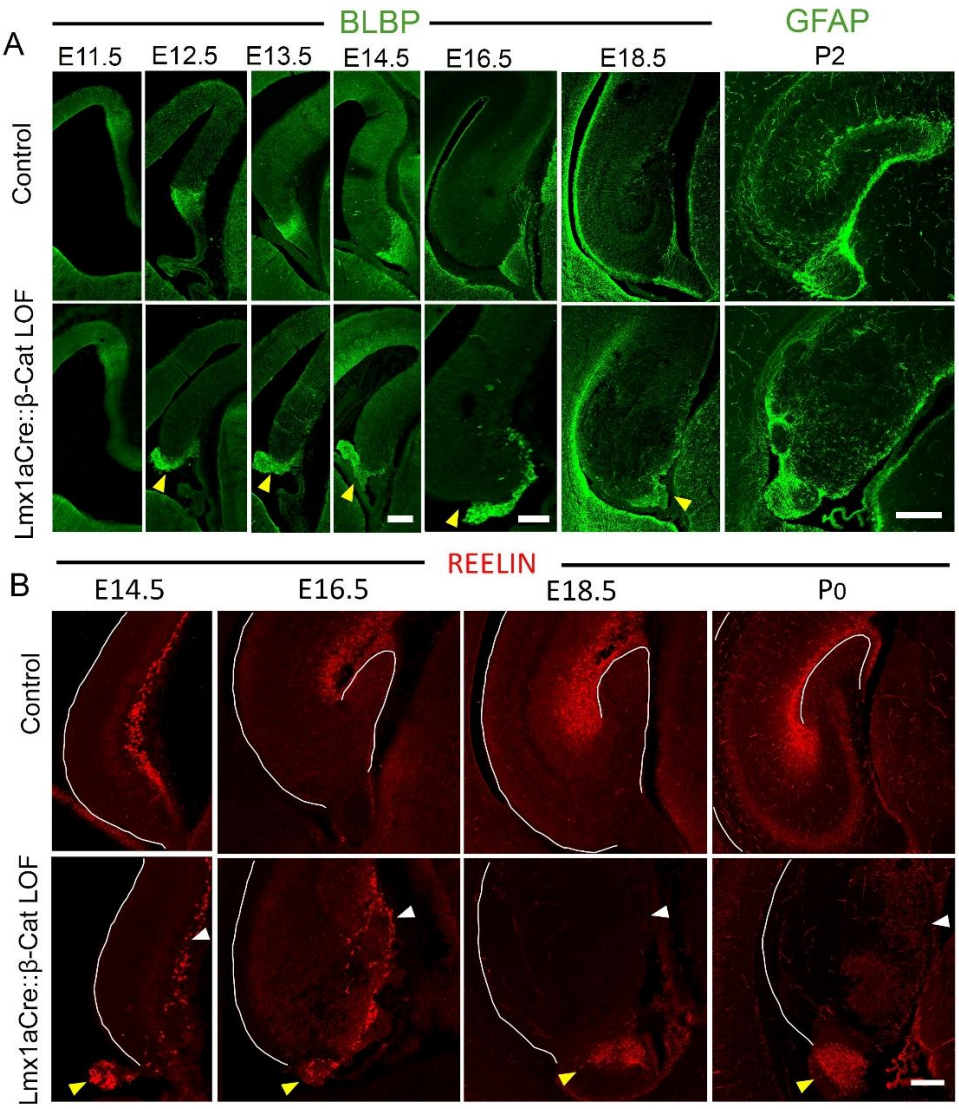

Fig. S2. No improvement of the β-Catenin LOF fimbrial scaffold disruption or CR cell mispositioning during late embryonic development. (A) BLBP (E11.5-E18.5) and GFAP (P2) immunolabeling show a well-organized fimbrial scaffold in controls, but a misoriented and disorganized scaffold in the Lmx1aCre::β-Catenin LOF brains; N=3 (E11.5) N=4 (E12.5); N=5 (E13.5 and E14.5), N=4 (E16.5 and E18.5), N=3 (P2) brains (biologically independent replicates) examined over 2 independent experiments. (B) Immunostaining for REELIN at E14.5, E16.5, E18.5 & P0 reveals no improvement in the mislocalized CR cells in the Lmx1aCre::β-Catenin LOF brains

during development (Marginal zone: white arrowheads, ectopic localization: yellow arrowheads); N=3 (E14.5); N=5 (E16.5), N=3 (E18.5), N=3 (P0) brains (biologically independent replicates) examined over 3 independent experiments. All scale bars: 100 μm.

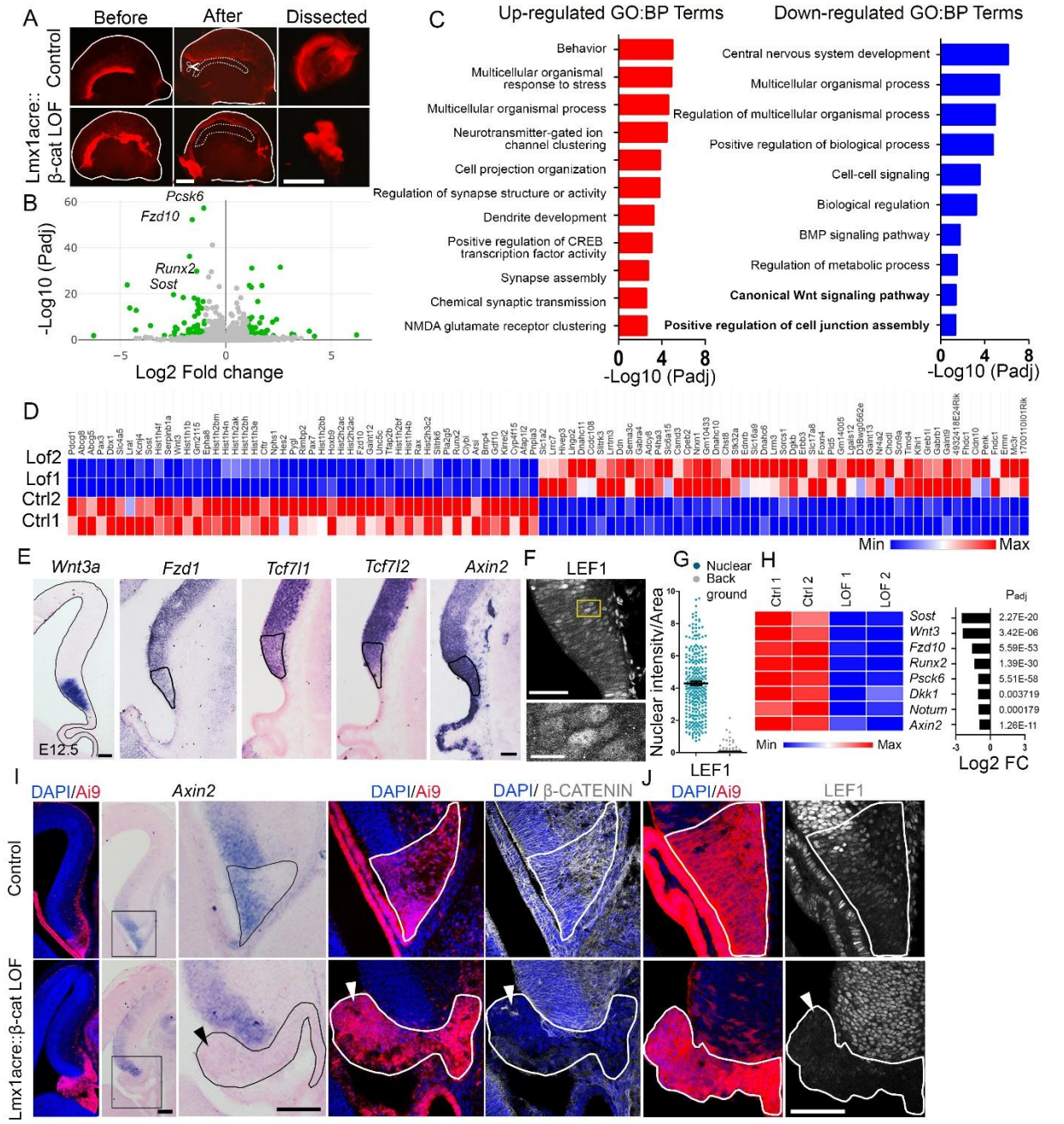

Fig. S3. Transcriptional changes associated with loss of β-CATENIN in the cortical hem. (A) Microdissection of E12.5 Ai9-labeled telencephalic hemispheres (before and after dissection) to obtain hem tissue for RNA sequencing. (B) A volcano plot showing differentially regulated genes (green dots represent genes with significantly changed expression). (C) Top 10 upregulated and downregulated GO: BP terms show down-regulation of “Canonical Wnt signaling pathway” and “Positive regulation of cell

junction assembly" in Lmx1aCre::β-Catenin LOF compared to controls. (D) Heat map representing Top 50 upregulated (red) and downregulated (blue) genes in control and Lmx1aCre::β-Catenin LOF brains; N=2 biological replicates. (E) The cortical hem, identified by *Wnt3a* expression, expresses several canonical Wnt pathway components such as *Fzd1, Tcf7l1, Tcf7l2*, and *Axin2* at E12.5, N=3 brains (biologically independent replicates) examined over 3 independent experiments. (F, G) immunostaining for Wnt target LEF1 and quantification. (H) Heatmap (displaying normalized reads) and Bar plots (showing log2 fold changes) of candidate Wnt pathway genes downregulated upon loss of β-CATENIN in the hem (complete data in supplementary table 1). (I) *In situ* hybridization for *Axin2* and immunolabeling for β-CATENIN in serial sections shows *Axin2* is undetectable (black arrowhead) at the same region where β-CATENIN staining is lost (Ai9 + area) in Lmx1aCre::β-Catenin LOF brains compared to controls. (J) LEF1 immunolabeling is almost undetectable (white outline) in Lmx1aCre::β-Catenin LOF hem (Ai9+ area). All scale bars: 100 μm.

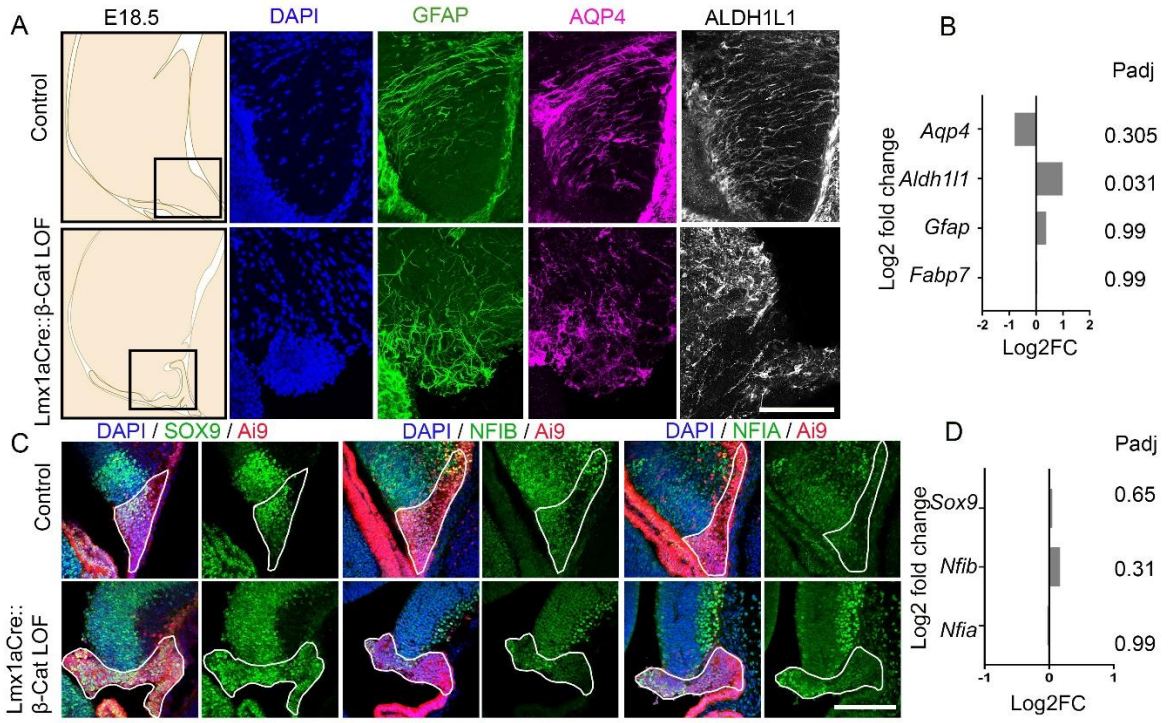

Fig. S4. Fimbrial scaffold markers and regulators maintain their expression upon loss of β-CATENIN. (A, B) The β-Catenin LOF fimbrial scaffold continues to display GFAP, AQP4, and ALDHL1 immunoreactivity (A), and expression of *Aqp4, Aldh1l1, Gfap, and Fabp7* is not significantly different (B) from that in control brains. (C) Immunostaining for SOX9, NFIA, and NFIB displays the presence of these regulators of fimbrial scaffold development and (D) Expression of *Sox9, Nfib, and Nfia* is not significantly altered in both control and β-Catenin LOF brains.

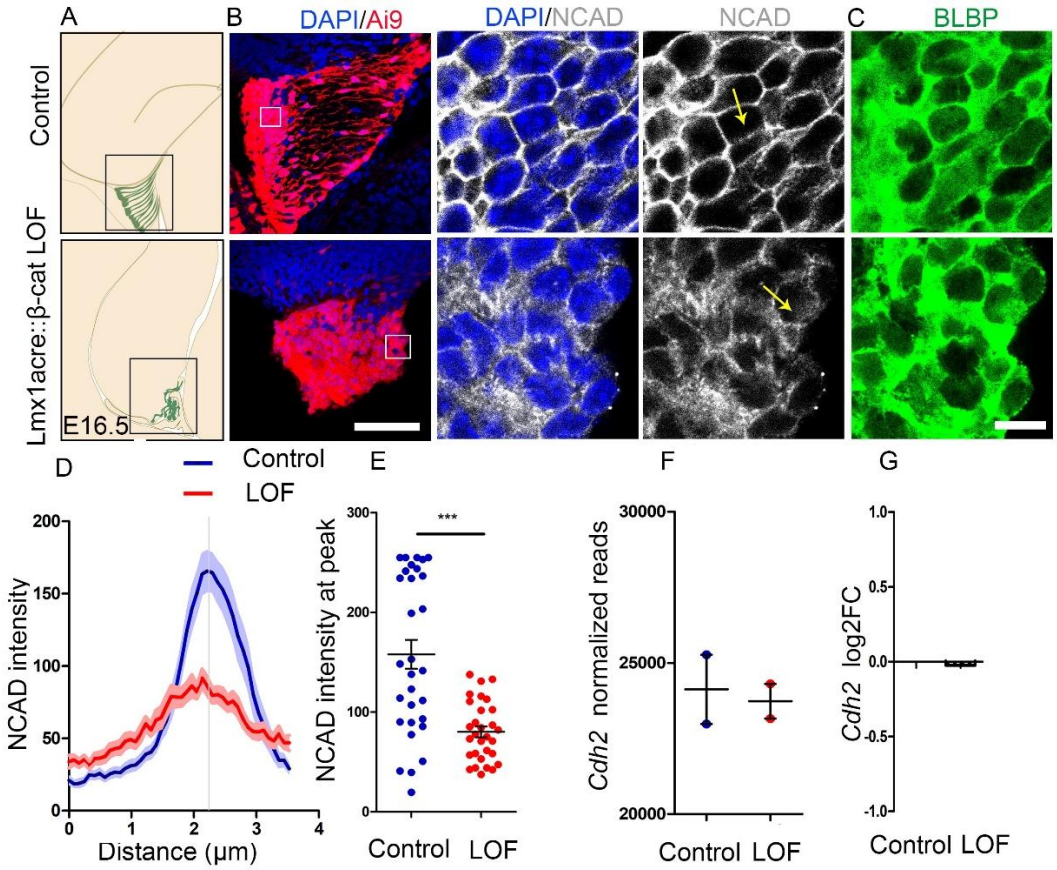

Fig. S5. Loss of β-CATENIN in cortical hem leads to altered cell-cell adhesion.

(A-C) Distribution of adherens junction marker N-CADHERIN and fimbrial scaffold marker BLBP in Ai9+ hem-derived cells. (B) High magnification images correspond to the boxed regions in the Ai9 image. (D, E) The intensity distribution of N-CADHERIN was quantitated across cell junctions (along the yellow arrow in the NCAD image). N= 3 brains (biologically independent replicates) examined over 3 independent experiments. (G) Normalized read counts (F) and log2 fold change for *Cdh2* gene, which encodes for NCAD, shows no significant change (p=0.99) between Lmx1aCre::β-Catenin LOF brains compared to controls. Statistical test: Two-tailed unpaired t-test with Welch correction (E) and Two-tailed unpaired Mann Whitney U test (D), * $p < 0.05$, ** $p < 0.01$, *** $p < 0.001$, ns if p-value> 0.05; P<0.0001 (E). Scale bars: 10 μm (C); 100 μm (B).

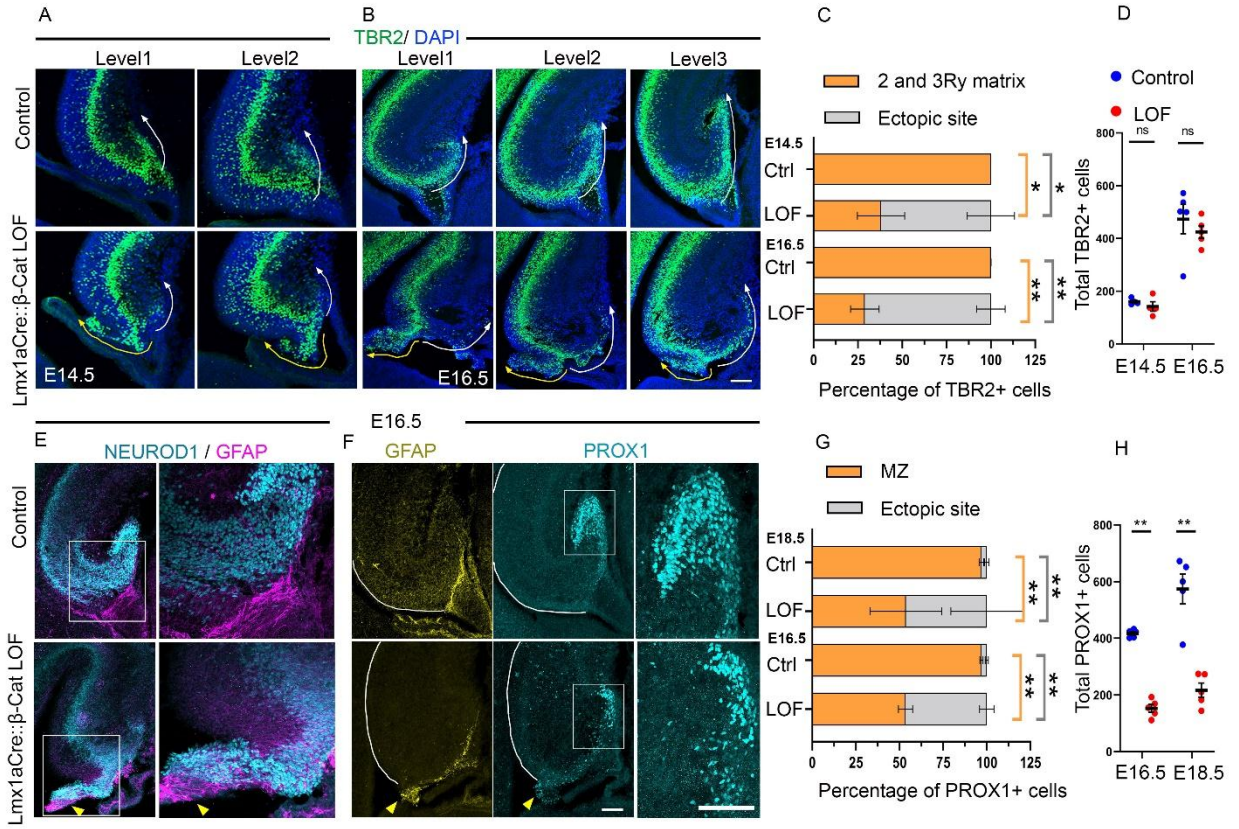

Fig. S6. The dentate migratory stream is diverted in the Lmx1aCre::β-Catenin LOF brains. (A, B) Sections at different rostro-caudal levels from E14.5 (A) and E16.5 (B) brains display TBR2+ cells in the 2ry & 3ry matrix of the dentate migratory stream in controls (white arrows). This migration is diverted to the ectopic glial protrusion in Lmx1aCre::β-Catenin LOF brains (yellow arrows). (C) Stacked percentage bar graphs displaying the altered distribution of TBR2+ dentate migratory cells in the 2ry & 3ry matrix vs the ectopic protrusion in Lmx1aCre::β-Catenin LOF brains compared to controls, N=4 (E14.5), N=5 (E16.5) brains (biologically independent replicates) examined over 3 independent experiments. (D) The total number of TBR2+ cells is not significantly different between Lmx1aCre::β-Catenin LOF and control brains. (E, F) At E16.5, Lmx1aCre::β-Catenin LOF brains display a disorganized GFAP+ fimbrial scaffold (yellow arrowheads) and mislocalized NEUROD1+ (E) and PROX1+ (F) dentate migratory cells. The boxed regions in E and F are shown at high magnification in the adjacent images. (G) Stacked percentage bar graphs displaying proportion of PROX1+

granule cells in the MZ (white box in F) vs the ectopic site (outside the white box) in the Lmx1aCre::β-Catenin LOF brains compared to controls, N=5 (E14.5 and E16.5) brains (biologically independent replicates) examined over 3 independent experiments. (H) The total number of PROX1+ granule cells is significantly lower in Lmx1aCre::β-Catenin LOF brains compared to controls. Stacked bar graphs (C and G) use the same data sets shown in the violin plots in Fig 3D and G. Error bars in C, D, G, and H represent SEM. Statistical test: Two-tailed unpaired Mann Whitney U test, * $p < 0.05$, ** $p < 0.01$, *** $p < 0.001$, ns if p-value> 0.05; P=0.028 (C, E14.5), P=0.0079 (C, E16.5), P=(0.3,E14.5; 0.15, E16.5), P= 0.007 (G, E16.5 and e18.5), and P=0.008 (H). All scale bars: 100 μm.

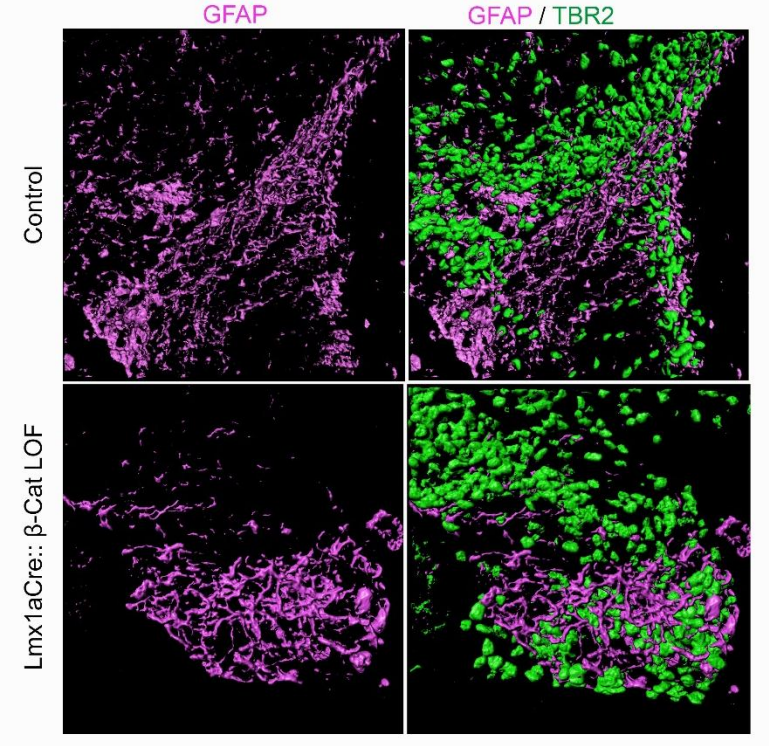

Fig. S7. A 3D reconstruction of the GFAP+ fimbrial scaffold and TBR2+ dentate migratory stream at E16.5. Upon loss of β-CATENIN the fimbrial scaffold is disorganized and the TBR2+ dentate migratory stream is diverted and intermingled with the disoriented fimbrial scaffold (see supplementary movie 1). Scale bar: 30μm.

Table S1. Normalized read counts and log2 fold changes with adjusted P values for the RNA seq data presented in Fig.S3, 4 & 5.

Click here to download Table S1

Supplementary dataset 1. Contains all the raw data points, statistical test summaries, and P value information corresponding to all the graphs shown in the main and the supplementary figures.

Click here to download Dataset 1

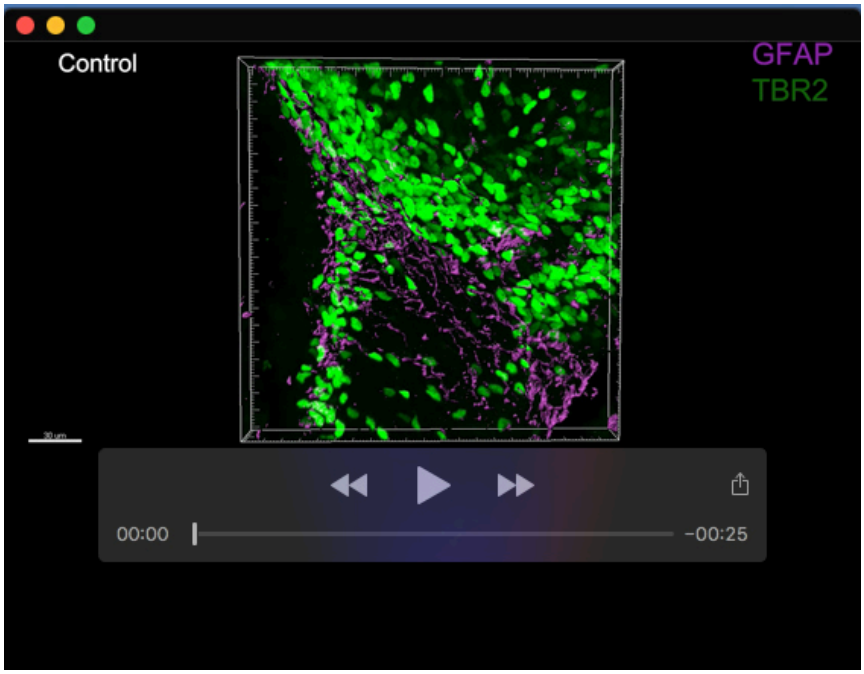

Movie 1. A movie corresponding to Fig. S7, generated using Imaris software, showing a 3D view of the GFAP+ fimbrial scaffold and the TBR2+ dentate migratory stream at E16.5. Loss of β-CATENIN leads to a disorganized fimbrial scaffold and diversion of the TBR2+ dentate migratory stream.